Journal of Solid State Chemistry 184 (2011) 2695–2700

Contents lists available at SciVerse ScienceDirect

Journal of Solid State Chemistry

journal homepage: www.elsevier.com/locate/jssc

Photoluminescence of samarium-doped TiO_2 nanotubes

Dong Jin Park [a], Tohru Sekino [a,*], Satoshi Tsukuda [a], Asuka Hayashi [b], Takafumi Kusunose [c], Shun-Ichiro Tanaka [a]

[a] Institute of Multidisciplinary Research for Advanced Materials (IMRAM), Tohoku University, Katahira 2-1-1, Aoba-ku, Sendai 980-8577, Japan
[b] The Institute of Scientific and Industrial Research (ISIR), Osaka University, 8-1, Mihogaoka, Ibaraki, Osaka 567-0047, Japan
[c] Faculty of Engineering, Kagawa University, Hayashi 2217-20, Takamatsu, Kagawa 761-0396, Japan

ARTICLE INFO

Article history:
Received 19 May 2011
Received in revised form
20 July 2011
Accepted 10 August 2011
Available online 16 August 2011

Keywords:
Titania nanotube
Rare earth
Photoluminescence
Doping
Soft chemical method
Energy transfer

ABSTRACT

Samarium (Sm)-modified TiO_2 nanotubes (TNTs) were synthesized by low-temperature soft chemical processing. X-ray powder diffraction analyses of the synthesized Sm-doped and non-doped TNTs show a broad peak near $2\theta=10^{\circ}$, which is typical of TNTs. The binding energy of Sm $^3d_{5/2}$ for 10 mol% Sm-doped TNT (1088.3 eV) was chemically shifted from that of Sm_2O_3 (1087.5 eV), showing that Sm existed in the TiO_2 lattice. Sm-doped TNTs clearly exhibited red fluorescence, corresponding to the doped Sm^{3+} ion in the TNT lattice. The Sm-doped TNT excitation spectrum exhibited a broad curve, which was similar to the UV–vis optical absorption spectrum. Thus, it was considered that the photoluminescence emission of Sm^{3+}-doped TNT with UV-light irradiation was caused by the energy transfer from the TNT matrix via the band-to-band excitation of TiO_2 to the Sm^{3+} ion.

1. Introduction

At present, the optoelectronic device and flat-panel display markets are expanding globally. The incorporation of rare earth (RE) elements in such devices depends on their luminescence behavior, and photophysical insights into their excited-state species through fundamental and applied studies are of paramount importance. As RE elements can be incorporated in glasses, metal oxides, phosphors, metal organic complexes, and various wide band-gap semiconductor materials, [1] they can be exploited in the design of materials for micro and nanoscale device applications.

Luminescence of materials depends on their electronic band structure. RE element ions are in the divalent or trivalent state and have intense luminescence because of 4*f* electron transitions. Hence, luminescence of RE elements is almost independent of the host matrix. However, the energy levels of RE elements could be largely influenced by the crystal symmetry, and this does depend on the host material. Therefore, the choice of host material is a very important factor for achieving good optical properties [1,2]. For these reasons, titanium dioxide (TiO_2), a wide band-gap (3.2 eV) semiconductor material that has attracted considerable attention because of its multiple potential applications, is a plausible candidate for the host material.

Recent investigations revealed that TiO_2 could be synthesized in tubular, wire-, and rod-like forms. Among them, titanium dioxide (TiO_2) nanotube (TNT) [3–5] having an one-dimensional nanostructure has attracted much attention not only in fundamental studies but also in application oriented investigations on, for example, gas sensors [6] and dye-sensitized solar cells [7]. We demonstrated that doping of TNT is advantageous in enhancing various physical and/or chemical properties; doping of transition metal cations such as Cr and Mn in TiO_2 nanotubes enhances the electrical conductivity and thermal stability of TNTs [5]. Furthermore, the doping of Sm to TNT enhances the molecular adsorption properties of TNT because of the modification of the TNT charge states by the trivalent Sm^{3+} ions in the TiO_2 lattice and the corresponding oxygen vacancies [8].

From these facts, it is expected that RE-doped TNTs also exhibit photoluminescence (PL). Zeng et al. [9] reported the PL properties of three kinds of Eu^{3+}-doped TiO_2 nanostructures and found stronger and longer lifetime PL emission from the Eu^{3+}-doped TNTs due to the energy transfer from TiO_2 to Eu^{3+} ions. However, detailed investigations on the PL properties including energy-transfer characteristics have not yet been reported for low-dimensional semiconductor oxide nanotubes doped with samarium (Sm). In this study, Sm^{3+}-doped TiO_2 nanotubes were synthesized by low-temperature soft chemical processing and their crystallinity, chemical compositions, nanostructures, and PL properties were investigated. Furthermore, we discuss the energy-transfer behavior in TiO_2 nanotubes in relation to

* Corresponding author. Fax: +81 22 217 5832.
E-mail address: sekino@tagen.tohoku.ac.jp (T. Sekino).

0022-4596/$ - see front matter © 2011 Elsevier Inc. All rights reserved.
doi:10.1016/j.jssc.2011.08.012

their PL characteristics and crystal field environment of doped Sm^{3+} ions.

2. Experimental procedure

2.1. Preparation of Sm-doped TNTs

TNTs were synthesized using a solution chemical process that was previously reported by Kasuga et al. [3,4]. Anatase-type TiO_2 powder (99.9%, Kojundo Chemical Laboratory Co. Ltd., Tokyo, Japan) and $Sm(NO_3)_3 \cdot 5H_2O$ (99.9%, Wako Pure Chemical Industries, Ltd., Osaka, Japan) were used as the starting materials. The molar concentrations of Sm were varied at 0%, 0.5%, 1%, 3%, 5%, and 10%. The weighted powders were added to 10 M NaOH aqueous solution in fluoropolymer bottles and ultrasonicated to disperse the powders homogeneously. The mixture was refluxed at 110 °C for 22 h, after which the product was washed with distilled water (DW) several times and neutralized with 0.1 M HCl. Next, the product was washed again with DW until the conductivity reached 10 μS/cm to eliminate the residual electrolytes such as sodium and chloride ions. The obtained powder was then filtered, rinsed with ethanol, and dried at 70 °C for 24 h. Finally, Sm-doped TiO_2 nanotubes were calcined at 400 °C for 3 h to eliminate structural water and hydroxyl groups and to increase its crystallinity.

2.2. Characterization

Synthesized nanotubes were investigated by an X-ray diffractometer (XRD: Cu *K*α ray, RINT2200, Rigaku Co., Tokyo, Japan) to identify the crystalline phase. Chemical composition analysis was carried out using an X-ray fluorescence spectrometer (ZSX100, Rh *K*α, Rigaku Co.). Transmission electron microscopy (TEM: 200 kV, JEM-2010, JEOL Ltd., Tokyo, Japan) and field-emission scanning electron microscopy (FE-SEM, S-4100, Hitachi Ltd., Tokyo, Japan) were used to investigate the nanostructure of the products. Samples for TEM investigation were prepared by dropping ethanol suspensions of the synthesized nanotubes on a carbon-coated Cu grid. X-ray photoelectron spectroscopy (XPS: Mg *K*α ray, 10 mA, 10 kV, ESCA3400, PHI-5600, Perkin-Elmer, OH, USA) was used to identify the existence and bonding states of elements in the synthesized nanotubes. Optical transmission spectra were measured using an ultraviolet-visible light spectrophotometer (UV–vis, V-650, JASCO, Tokyo, Japan) in a wavelength range from 200 to 600 nm. PL measurement was performed using a fluorescence spectrometer (FP-6600, JASCO Corp., Tokyo, Japan) for the Sm-doped samples.

3. Results and discussion

3.1. Crystalline phase and chemical compositions

To investigate the crystalline structure of the Sm-doped TNTs, XRD measurements were performed, the results of which are shown in Fig. 1 along with that of non-doped TNT. For the non-doped sample, the broad peaks around 2θ of 24°, 28°, 48°, and 62° are from the titanate nanotubes containing H^+ and/or Na^+ ions [10–12]. The broad peak around $2\theta = 10°$ corresponds to the layer spacing in the nanotube wall; it is argued that the TiO_2 nanotube is formed by scrolling titanate nanosheets composed of $H_2Ti_3O_7$, $Na_xH_{2-x}Ti_3O_7$ or lepidocrocite-type $A_xTi_{2-x/4}\square_{x/4}O_4$ (A; Na and/or H, □; vacancy) crystals that have a layered structure. The scrolling direction of the wall had been proposed to occur along the (100) plane and could occur around the [001] axis [13,14]. Furthermore,

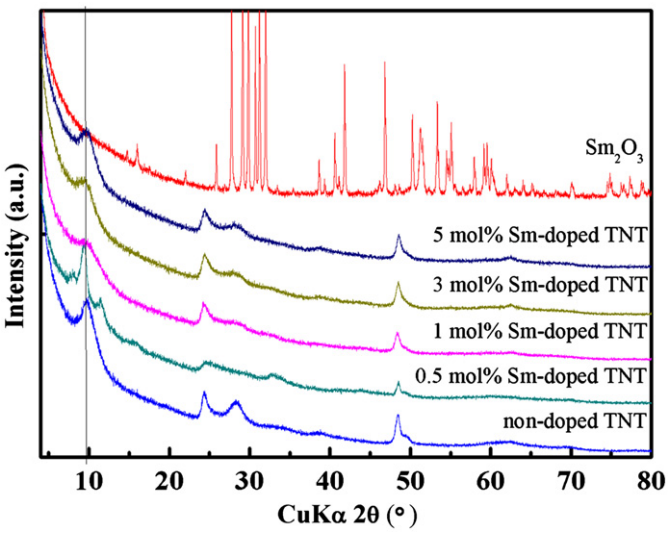

Fig. 1. XRD patterns for pure Sm_2O_3 powder and the Sm-doped TNTs with addition of Sm of molar concentrations from 0% to 5%.

Table 1
Sm contents in doped-TNTs analyzed by XRF measurement for 0.5–10 mol% of nominal Sm contents.

Samples (mol% of Sm)	0.5	1	2	3	5	10
Analyzed Sm content						
In mol%	0.13	0.50	0.56	1.0	2.2	1.2
In mass%	0.70	2.7	2.9	5.2	10	4.7

it should be noted that these crystal structures consists of TiO_6 octahedra, which have similar coordination environment to the anatase- and rutile-types of TiO_2. In the Sm-doped sample, the peak at around $2\theta = 10°$ was also observed and the overall XRD pattern was similar to that of non-doped TNT, indicating that the nanotubes formed in the presence of Sm. However, the Sm-doped TNTs showed a broader XRD profile than that of the non-doped TNT, and in addition, the peak around 10° slightly shifted towards a lower diffraction angle. These results indicate that the layer distance of the titanate crystals in the walls of the nanotube were shortened by Sm addition. Furthermore, no Sm_2O_3 pattern was observed in the synthesized Sm-doped TNTs by XRD analysis (Fig. 1).

Elemental analysis using X-ray fluorescence confirms the presence of Sm in the synthesized TiO_2 nanotubes (Table 1), even at low Sm concentrations (0.13–2.2 mol%, cf. nominal compositions 0.5–10 mol%). It is considered that some Sm might be dissolved during synthesis. In addition, Na was not found in the TNT samples, showing the obtained TNTs consisted of Ti, O, and Sm.

3.2. Nanostructure characteristics

The morphology of non-doped and Sm-doped TNTs was observed by SEM and TEM. The TEM images, shown in Fig. 2, revealed that nanotubular structures of non-doped TiO_2 formed with diameters of approximately 10 nm and length of several hundreds of nanometers. The Sm-doped TiO_2 nanotubes were of similar morphology. However, slightly larger diameter, approximately 16 nm for the 1 mol% Sm-doped TNT (Fig. 2b), was confirmed for the Sm-doped samples.

SEM images for the Sm-doped TNTs showed that the tubes were entangled with each other and formed large agglomerates (Fig. 3a). However, no TNT surface particulates were observed by SEM analysis as well as by TEM investigation. As mentioned

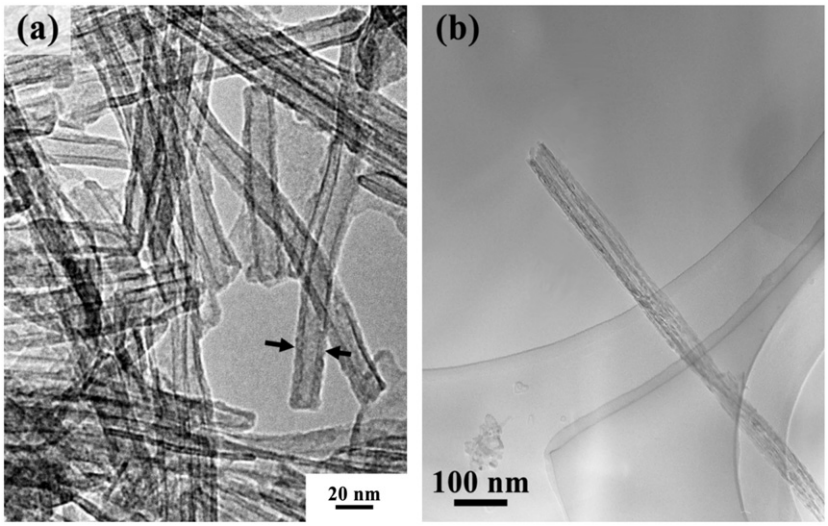

Fig. 2. TEM images of (a) non-doped TNT showing a tubular structure with a length of over 800 nm and (b) high magnification image of 1 mol% Sm-doped TNT. Arrows in (a) represents typical diameter (10.2 nm) for non-doped TNT.

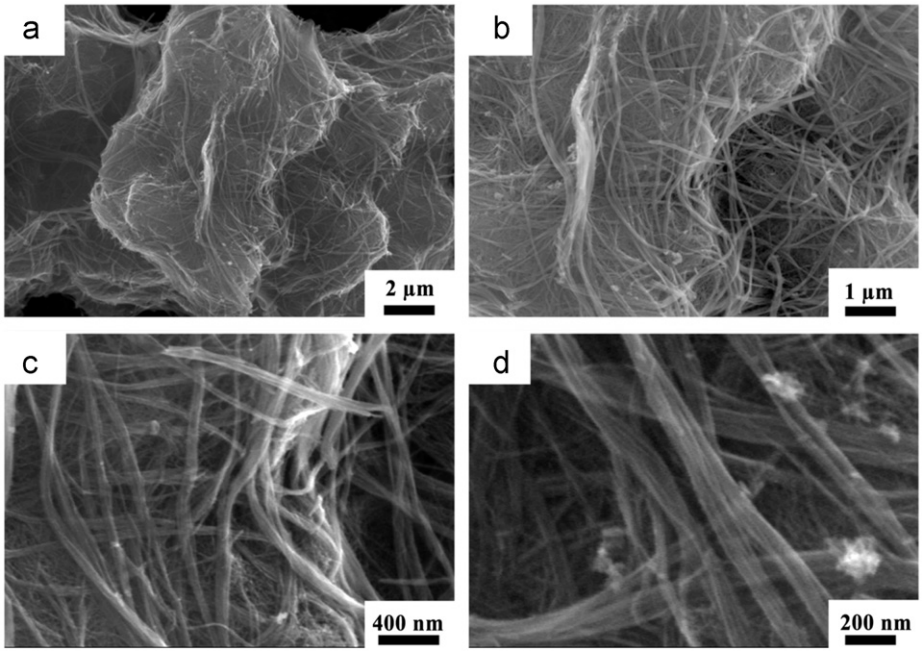

Fig. 3. FE-SEM images of 1 mol% Sm-doped TNT taken at different magnifications (a) ×5 k, (b) ×10 k, (c) ×30 k, and (d) ×50 k.

before, no crystalline Sm_2O_3 was confirmed in XRD analysis while Sm was detected in the XRF measurements of the synthesized samples; therefore, it is inferred that Sm is well doped in the crystalline lattice of TiO_2 nanotubes.

3.3. Photoluminescence properties

PL emission spectra of the Sm-doped TNTs were obtained in the range 400–700 nm. The PL emission spectrum for the 1 mol% Sm-doped TNT shown in Fig. 4(b) exhibits strong red fluorescence with 350-nm excitation, which could also be clearly visible by naked eyes. Furthermore, the shape and peak position of the PL spectra for the 3 and 5 mol% Sm-doped TNTs were the same as those of 1 mol% sample, except the PL intensity; the PL emission intensity increased with increase in Sm content.

The emission spectrum exhibits three major peaks at 580 nm, 610 nm, and 660 nm that correspond to $^4G_{5/2} \rightarrow {}^6H_{5/2}$, $^4G_{5/2} \rightarrow {}^6H_{7/2}$, and $^4G_{5/2} \rightarrow {}^6H_{9/2}$ *f–f* transitions of the Sm^{3+} in the $4f^5$ configuration, respectively. These results are in good agreement with the previous reports on the PL characteristics of Sm^{3+} [15–20], and thus, it is confirmed that Sm-doped TNT exhibits photoluminescence because of the doped Sm^{3+} ion.

The PL of RE-doped mesoporous TiO_2 films was first reported by Frindell et al. [19], who proposed that the efficient energy-transfer process from the TiO_2 lattice conduction band to the RE ion via the TiO_2 surface defects results in PL emission from RE-doped TiO_2 film in the visible range. Recently, Jing et al. [20] reported the detailed PL properties and the energy-transfer characteristics for Sm^{3+}-doped anatase- and rutile-types TiO_2 thin films. They explained that the PL emission originated from the indirect excitation of the Sm^{3+} ions through the energy

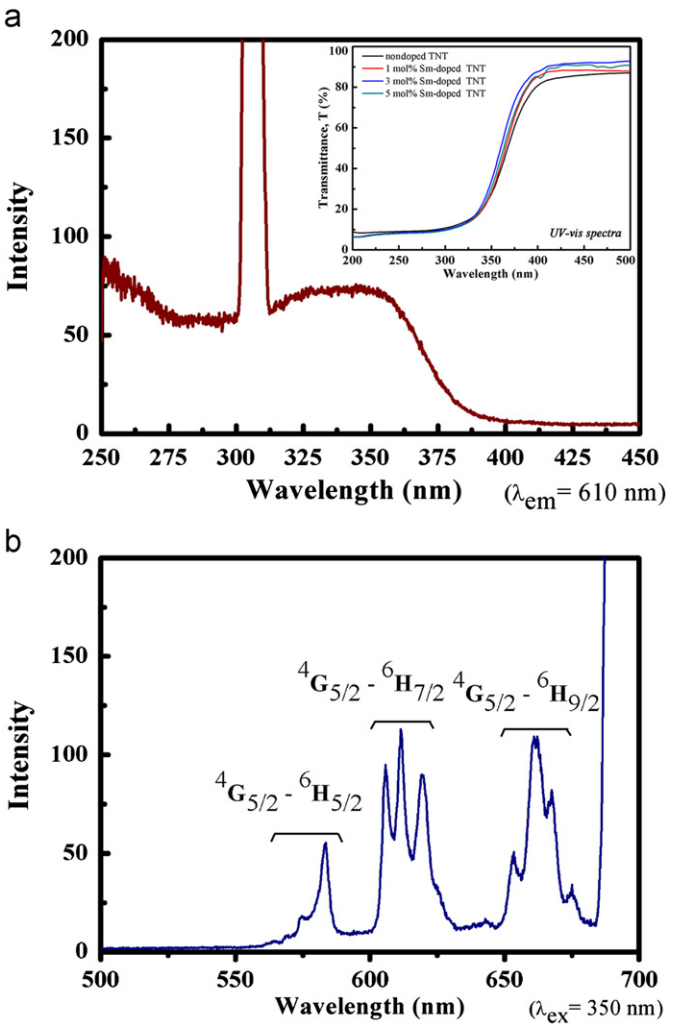

Fig. 4. PL spectra of 1 mol% Sm-doped TNT (a) excitation spectra (monitored at 610 nm. Rayleigh scattered peak presents at 305 nm) and (b) emission spectra (excited at 350 nm). The inset in 5(a) shows the UV–vis transmission spectra.

transfer from electron–hole pairs created in the TiO_2 host; however, they claimed that the energy transfer from the conduction band of the TiO_2 host lattice is not via the defect state of the host lattice but occurs directly to the $^4G_{5/2}$ inner core level of the Sm^{3+} ions and then to the ^6H_J levels (J=5/2, 7/2, 9/2, and 11/2) with visible light emission. Jing et al. [20] also pointed out that the fine structure in the PL emissions appeared at the high energy side at around 575 nm of the $^4G_{5/2}\rightarrow{}^6H_{5/2}$ transition, which can also be observed in the present Sm-doped TiO_2 nanotubes (see Fig. 4b, 563–575 nm). In addition, the transitions to $^6H_{7/2}$ and $^6H_{9/2}$ also accompany several peaks. These fine structures in the PL spectrum can be attributed to the Stark effect; it was reported that the Sm-doped glasses exhibited several fluorescence transitions between various energy levels, which were associated by the Stark splitting of each energy levels, such as ^6H_J, ^4G_J. and $^4F_{3/2}$, of Sm^{3+} ions in the glass hosts [21]. In more detail, because the $^6H_{5/2}$ level is the ground state of the Sm^{3+} ions and is split into three levels when the ions are in a non-cubic crystal field [16,20], which might be the case for the distorted MO_6 octahedron in the anatase structure.

Contrary to the emission spectrum, the excitation spectrum, shown in Fig. 4a, shows a broad curve without obvious peaks. It is quite similar to the UV–vis optical absorption spectrum (inset in Fig. 4a), demonstrating that the excitation of Sm-doped TNT follows the absorption edge of TiO_2. When the RE ions are directly excited, both the emission and excitation spectra should have sharp peaks and be rather symmetrical according to the corresponding energy levels. However, as this is not the case here, it indicates that the PL emission originates from the indirect excitation of Sm^{3+} via energy transfer from the excited TiO_2 nanotube lattice to the doped Sm^{3+} ions, a phenomenon which occurs in Sm-doped TiO_2 thin films [19,20].

The well-resolved PL spectrum of the Sm-doped TNT clearly demonstrates that the Sm^{3+} ions are located in a regular crystal field environment. The PL characteristics of RE ions in a crystal field depend on the symmetry of the coordination structure, and lead to a splitting of the energy levels. In the TiO_2 nanotube doped with Sm^{3+} ions, although the radius of the Sm^{3+} ion (0.96 Å) is larger than that of the Ti^{4+} ions (0.605 Å), it can be concluded that the Sm^{3+} ions substitute the Ti^{4+} ions in the TiO_2 nanotubes lattice. In addition, they distort the $Ti(Sm)O_6$ octahedral structure due to the large ionic radius difference and the formation of oxygen vacancy by the substitution of trivalent (Sm^{3+}) ions to tetravalent (Ti^{4+}) ones. All these facts are regarded to have influence on the resulting PL properties of the Sm-doped TNTs. Furthermore, the charge recombination analysis using time-resolved diffuse reflectance spectroscopy revealed that the non-doped pure TNT exhibited remarkably long lifetime of photo-induced charges such as electron than that of TiO_2 nanoparticles

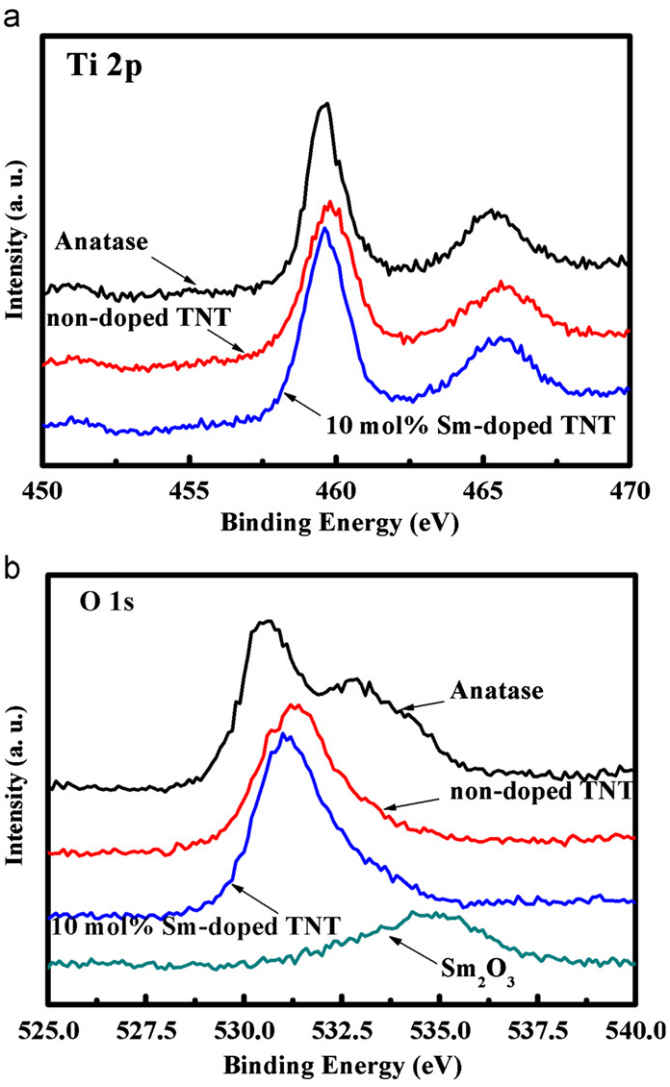

Fig. 5. XPS spectra of (a) Ti $2p_{3/2}$ and $2p_{1/2}$ and (b) O 1*s* in 10 mol% Sm-doped TNT.

due to the longer diffusion length [22], showing the advantage of one-dimensional (1D) nanostructured TiO_2 in charge transport behavior. It is therefore inferred that the strong PL in the present Sm-doped TNT is associated with the effective energy transfer from TNT lattice to Sm^{3+} ions owing to the long lifetime of photoinduced charges in the unique 1D semiconductor host. More detailed investigation regarding energy transport dynamics as well as PL emission kinetics for the Sm-doped TNTs will be the subject of future reports.

3.4. XPS spectra analysis

XPS measurements were performed to confirm the existence and bonding nature of the Sm^{3+} ions in TiO_2 nanotubes. Figs. 5 and 6 show the individual XPS spectra of TiO_2 anatase, non-doped TNT, Sm_2O_3, and 10 mol% Sm-doped TNT. The peaks of Ti, O, and Sm are observed. The peaks located at 459.1 and 464.9 eV indicate the spin–obit splitting of the Ti 2*p* components ($2p_{3/2}$ and $2p_{1/2}$, respectively), the peak at 530.6 eV is attributed to the O 1*s* component. These are in good agreement with those of the titanium dioxide species. The peak of C 1*s* at 285.4 eV is due to the absorbed carbon, and was used to calibrate the binding energy of the obtained spectra.

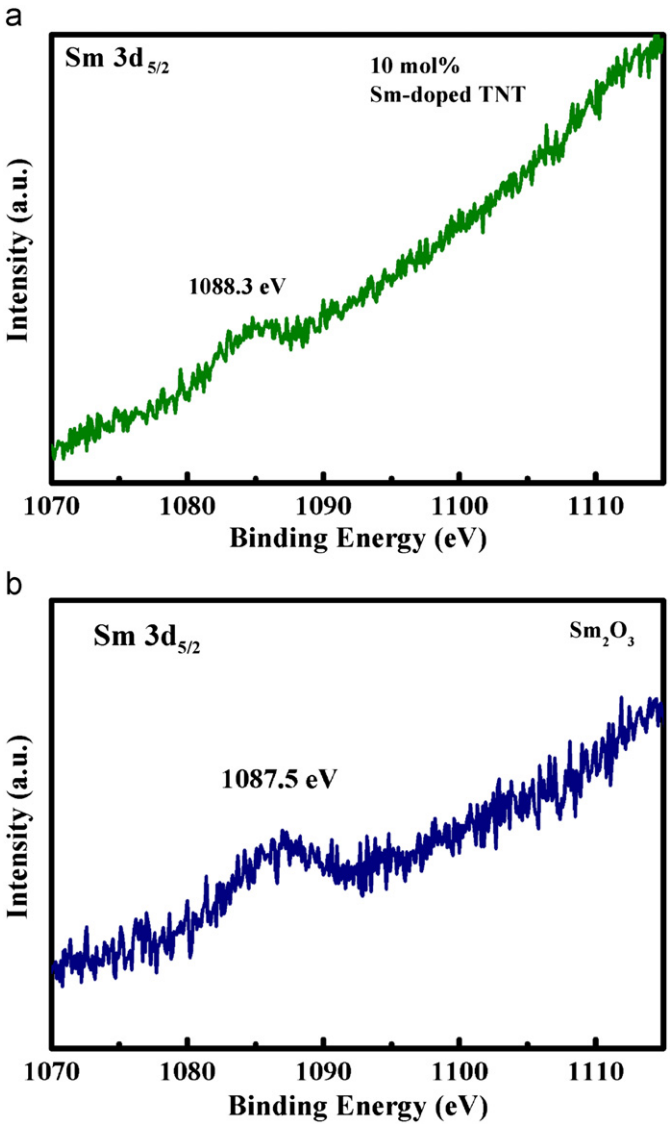

Fig. 6. XPS spectra of Sm $3d_{5/2}$ in (a) 10 mol% Sm-doped TNT, (b) Sm_2O_3, and (c) O 1*s* in Sm_2O_3 powder.

The peak at 1088 eV in Fig. 6(a) and (b) is attributed to the Sm $3d_{5/2}$ observed in Sm-TNT and pure Sm_2O_3 powder, respectively. The binding energy of Sm $3d_{5/2}$ in Sm-doped TiO_2 nanotubes (1088.3 eV) is slightly greater than that of Sm_2O_3 (1087.5 eV), corresponding to a chemical shift of 0.8 eV. Sm_2O_3 is a type-B monoclinic structure in which the Sm^{3+} ion bonds with seven oxygen atoms [23]. The chemical shift of Sm $3d_{5/2}$ is attributed to the difference in the chemical and coordination environments of the Sm^{3+} ions in the TiO_2 matrix; the binding energy in the 6-coordination environment of Sm^{3+} in the TiO_2 crystal is larger than that of the 7-coordination in the Sm_2O_3 crystal. From these XPS results, it is inferred that Sm^{3+} ions substitute Ti^{4+} ions in the TNTs and are located in a MO_6 octahedral crystal field environment, which agrees well with the results obtained from photoluminescence analysis.

4. Conclusion

TiO_2 nanotube was successfully modified by Sm doping through soft chemical process. The typical XRD peak of TNTs around $2\theta = 10^\circ$ was slightly shifted by the addition of Sm. The doping of Sm^{3+} ions in the TNT resulted in red photoluminescence. Energy transfer from the TNT matrix to the doped Sm^{3+} ions occurred via the band-to-band excitation of the TiO_2 lattice by incident light irradiation followed by the excitation of the doped Sm^{3+} ions resulting in Sm^{3+} fluorescence. XPS analysis also revealed that Sm^{3+} ions replaced the Ti^{4+} ions in the TNT lattice. It is concluded that the doping of appropriate elements such as Sm is advantageous to functionalize semiconductor oxide nanotube materials.

Acknowledgments

This work was partly supported by the Global COE (Center of Excellence) Program "Materials Integration, International Center of Education and Research, Tohoku University," MEXT, Japan, and by the Japan Society for the Promotion of Science (JSPS) under the Grant-in-Aid for Scientific Research (A). The authors gratefully acknowledge Prof. M. Kakihana and Dr. S. Tezsuka for their support in conducting the photoluminescence measurements.

References

[1] K.L. Frindell, M.H. Bartl, A. Popitsch, G.D. Stucky, Angew. Chem. Int. Ed. 41 (2002) 959–962.
[2] A. Conde-Gallardo, M. García-Rocha, I. Hernández-Calderón, R. Palomino-Merino, Appl. Phys. Lett. 78 (2001) 3436–3438.
[3] T. Kasuga, M. Hiramatsu, A. Hoson, T. Sekino, K. Niihara, Langmuir 14 (1998) 3160–3163.
[4] T. Kasuga, M. Hiramatsu, A. Hoson, T. Sekino, K. Niihara, Adv. Mater. 11 (1999) 1307–1311.
[5] T. Sekino, T. Okamoto, T. Kasuga, T. Kusunose, T. Nakayama, K. Niihara, Key Eng. Mater. 317–318 (2006) 251–254.
[6] L. Feng, Y. Liu, J. Hu, Langmuir 20 (2004) 1786–1790.
[7] S. Ushiroda, N. Ruzycki, Y. Lu, M.T. Spitler, B.A. Parkinson, J. Am. Chem. Soc. 127 (2005) 5158–5168.
[8] D.J. Park, T. Sekino, S. Tsukuda, S.-I. Tanaka, Synthesis of Sm-doped TiO_2 nanotube and analysis of its methylene blue removal properties under dark and UV irradiated conditions, Res. Chem. Intermed, in print.
[9] Q.G. Zeng, Z.M. Zhang, Z.J. Ding, Y. Wang, Y.Q. Sheng, Scr. Mater. 57 (2007) 897–900.
[10] J. Yu, H. Yu, B. Cheng, C. Trapalis, Nanotechnology 19 (2008) 045606.
[11] G.H. Du, Q. Chen, R.C. Che, Z.Y. Yuan, L.-M. Peng, Appl. Phys. Lett. 79 (2001) 3702–3704.
[12] R. Ma, Y. Bando, T. Sasaki, Chem. Phys. Lett. 380 (2003) 577–582.
[13] D.V. Bavykin, J.M. Friedrich, F.C. Walsh, Adv. Mater. 18 (2006) 2807–2824.
[14] W. Wang, O.K. Varghese, M. Paulose, C.A. Grimes, J. Mater. Res. 19 (2004) 417–422.

[15] V. Kiisk, I. Sildos, S. Lange, V. Reedo, T. Tätte, M. Kirm, J. Aarik, Appl. Surf. Sci. 247 (2005) 412–417.
[16] Z. Assefa, R.G. Haire, P.E. Raison, Spectrochim. Acta, Part A 60 (2004) 89–95.
[17] L. Hu, H. Song, G. Pan, B. Yan, R. Qin, Q. Dai, L. Fan, S. Li, X. Bai, J. Lumin. 127 (2007) 371–376.
[18] V. Kiisk, M. Savel, V. Reedo, A. Lukner, I. Sildos, Phys. Proc. 2 (2009) 527–538.
[19] K.L. Frindell, M.H. Bartl, M. Robinson, G.C. Bazan, J. Solid State Chem. 172 (2003) 81–88.
[20] F. Jing, S. Harako, S. Komuro, X. Zhao, J. Phys. D: Appl. Phys. 42 (8) (2009) 085109.
[21] B. Sharma, J. Vipin Prasad, S.B. Rai, D.K. Rai, Solid State Commun. 93 (1995) 623–628.
[22] T. Tachikawa, S. Tojo, M. Fujitsuka, T. Sekino, T. Majima, J. Phys. Chem. B 110 (2006) 14055–14059.
[23] H.R. Hoekstra, Inorg. Chem. 5 (1966) 754–757.